

## MEMS-based dynamic cell-to-cell culture platforms using electrochemical surface modifications

This article has been downloaded from IOPscience. Please scroll down to see the full text article.

2011 J. Micromech. Microeng. 21 054028

(<http://iopscience.iop.org/0960-1317/21/5/054028>)

View [the table of contents for this issue](#), or go to the [journal homepage](#) for more

Download details:

IP Address: 169.229.32.137

The article was downloaded on 29/04/2011 at 01:45

Please note that [terms and conditions apply](#).

# MEMS-based dynamic cell-to-cell culture platforms using electrochemical surface modifications

Jiyoung Chang<sup>1</sup>, Sang-Hee Yoon<sup>2</sup>, Mohammad R K Mofrad<sup>2</sup> and Liwei Lin<sup>1</sup>

<sup>1</sup> Berkeley Sensor and Actuator Center, Mechanical Engineering Department, University of California, Berkeley, CA, USA

<sup>2</sup> Bioengineering Department, University of California, Berkeley, CA, USA

E-mail: [lwlin@me.berkeley.edu](mailto:lwlin@me.berkeley.edu)

Received 1 November 2010, in final form 11 January 2011

Published 28 April 2011

Online at [stacks.iop.org/JMM/21/054028](http://stacks.iop.org/JMM/21/054028)

## Abstract

MEMS-based biological platforms with the capability of both spatial placements and time releases of living cells for cell-to-cell culture experiments have been designed and demonstrated utilizing electrochemical surface modification effects. The spatial placement is accomplished by electrochemical surface modification of substrate surfaces to be either adhesive or non-adhesive for living cells. The time control is achieved by the electrical activation of the selective indium tin oxide co-culture electrode to allow the migration of living cells onto the electrode to start the cell-to-cell culture studies. Prototype devices have a three-electrode design with an electrode size of  $50 \times 50 \mu\text{m}^2$  and the separation gaps of  $2 \mu\text{m}$  between them. An electrical voltage of  $-1.5 \text{ V}$  has been used to activate the electrodes independently and sequentially to demonstrate the dynamic cell-to-cell culture experiments of NIH 3T3 fibroblast and Madin Darby canine kidney cells. As such, this MEMS platform could be a basic yet versatile tool to characterize transient cell-to-cell interactions.

## 1. Introduction

Interactions between either the same or different types of living cells trigger a variety of unique cellular behavior, such as growth, migration and differentiation, to name a few. Therefore, it is desirable to engineer and dynamically characterize *in vitro* cell-to-cell interactions toward the understanding of *in vivo* responses of different living cells. However, handling and positioning living cells with both good temporal and spatial controls has been a fundamental issue as *in vitro* studies require seating of living cells on substrates. Previously, efforts have been introduced to study cell-to-cell interactions without the temporal control. For example, many groups have demonstrated the capability to place cells at specific locations with various patterns by using photolithography-based processes [1, 2]. Researchers have demonstrated that the usage of soft lithography can pattern cells reliably [3–5]. However, these lithography-based methods typically allow static patterning of living cells only without temporal control. Microfluidic technology has also

been applied to achieve cell patterning and placements [6]. A functional surface such as a thermally responsive polymer [7] (adhesive to non-adhesive surfaces for cells) is another approach toward cell-to-cell studies in a single platform. One drawback of this approach is the limitation on the selection and control of various temperature reactive polymers for different cell types. In a recent work, static placement of the living cells with in-plane structure by PEG (polyethylene glycol) silane has been demonstrated [8] without the temporal control. These and other previous demonstrations build up a strong foundation for our current work to construct dynamic cell-to-cell culture platforms.

Dynamic cell-to-cell culture processes to mimic *in vivo* cell behavior could provide better platforms for cell studies as they are one step closer to the real cellular environment as compared with single-cell studies. Some of the recent works have utilized the advanced MEMS fabrication technologies. For example, micromechanical control of cell-to-cell interaction by using MEMS actuators has been shown to reveal an unknown property between cells

[9]. This study utilized moving comb-shaped structures to manually control the culture platform by generating various gaps between two different types of cells for transient cellular studies. Electrochemical desorption of a SAM (self-assembled monolayer) with multi-types of cell-to-cell studies has also been demonstrated [10]. Efforts in combining micro contact printing and photoelectroactive surface chemistry is another approach to selectively release cells on specific areas [11]. These aforementioned methods have provided good fundamental understanding of transient behavior during cell-to-cell interactions, while further investigations could provide advanced knowledge for the signal pathways in multicellular domains.

Here, we propose a MEMS platform with the capabilities of both temporal and spatial control of living cells for the study of dynamic cell-to-cell interactions. Two types of cell lines (MDCK and NIH 3T3) have been utilized in this work to demonstrate the effectiveness of the proposed platform in multicellular cell-to-cell co-culture studies in contrast to the previous single-type cell-to-cell culture demonstrations [12]. This micro platform allows serial activations of electrodes to dynamically modify cell culture areas to enable possible future cellular studies, including the geometric surface impact on cell migration, biochemistry and mechanical signaling, and biological development during the cell-to-cell co-culture processes.

## 2. Working principle and fabrication

### 2.1. Working principle

Figure 1 illustrates the sequential steps on the proposed cell-to-cell co-culture platform using a three-electrode design. Only the key components were drawn and some of the typical elements such as interconnection wires to the electrodes were not shown to simplify the schematic diagram. The basic principle is to activate the ITO (indium tin oxide) electrode in sequence using electro-chemical effects, and a three-electrode design is shown as an example. A surface passivation process is conducted on the whole substrate to coat a layer of PEG (polyethylene glycol) silane which creates a covalent bond with the Pyrex substrate and the electrodes made of ITO. The anti-cell adhesive property of the long PEG-silane chain inhibits cell adhesion (surface deactivation process). When the individual ITO electrode is electrically activated at  $-1.5$  V for 45 s [8], the PEG layer is removed from the specific electrode to allow the seating of living cells only on the selective site (surface activation process). Figure 1(a) shows that the seating of the first cell type has already been accomplished for the electrode on the left-hand side (electrode 1). By repeating this process, a different type of living cell can be loaded on the opposite electrode (electrode 3) at the right-hand side as shown in figure 1(b) to accomplish spatial patterning of multi-types of living cells on the single platform. The gap between the adjacent ITO electrodes is lithographically controlled as  $2 \mu\text{m}$  in the prototype experiments which is small enough to allow the migration of living cells [13]. In the prototype fabrication, the lift-off process was used for the ITO deposition

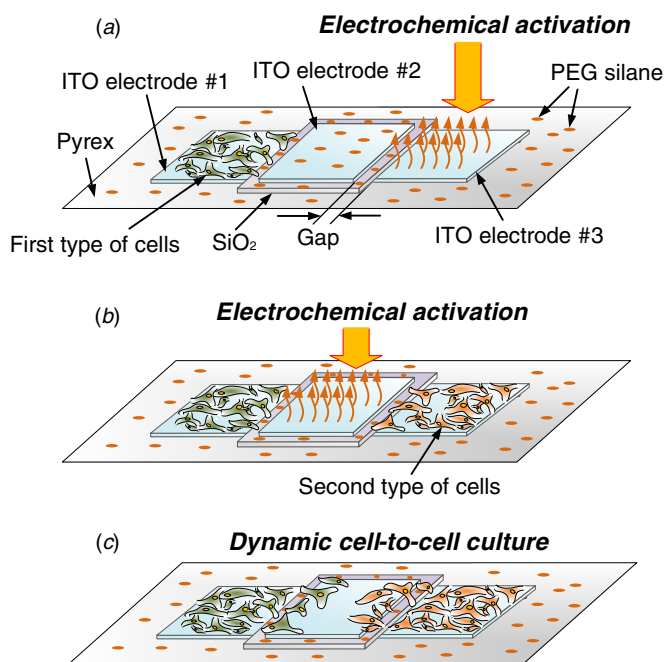


**Figure 1.** Schematic view of the working principle of the platform using a three-electrode system. First, the whole surface is covered with functionalized chemical, PEG (polyethylene glycol) silane. An individual ITO electrode surface is activated sequentially by applying a negative potential of 1.5 V for 45 s which activates the specific electrode to allow seating of living cells due to the selective desorption of PEG silane. (a) Seating of cell 1 on the left electrode was accomplished and the electrochemical activation of the right electrode. (b) Seating of cell 2 on the right electrode was accomplished and the electrochemical activation of the center electrode. (c) Living cells overcome the barrier gap and migrate into newly activated center electrode for cell-to-cell co-culture studies.

and patterning and the gap resolution was larger than the target value of  $2 \mu\text{m}$ . In order to control the gap size to be close to  $2 \mu\text{m}$ , the passivation oxide layer as shown in figure 1(a) was used under the center electrode (electrode 2) as a buffer. A second ITO layer was deposited on top of the buffer layer to construct the center electrode to have better control of the gaps between adjacent electrodes. The temporal control starts by activating the cell-to-cell co-culture electrode (center electrode or electrode 2) after the left and right electrodes were seated with living cells. Once the center electrode is activated by removing PEG silane, living cells on both sides can migrate into the center electrode as shown in figure 1(c).

### 2.2. Device fabrication

Figure 2 shows the sequential steps of the fabrication process. A Pyrex wafer was chosen as the substrate for its chemical inertness and outstanding optical transparency. A 150 nm-thick ITO layer was sputtered by dc sputtering and patterned using the lift-off process to define electrical connection lines, contact pads and cell culture electrode areas as shown in figure 2(a). After the sputtering process, annealing at  $350^\circ\text{C}$  for 1 h was performed to obtain reliable ITO film properties. The corresponding sheet resistance of the ITO

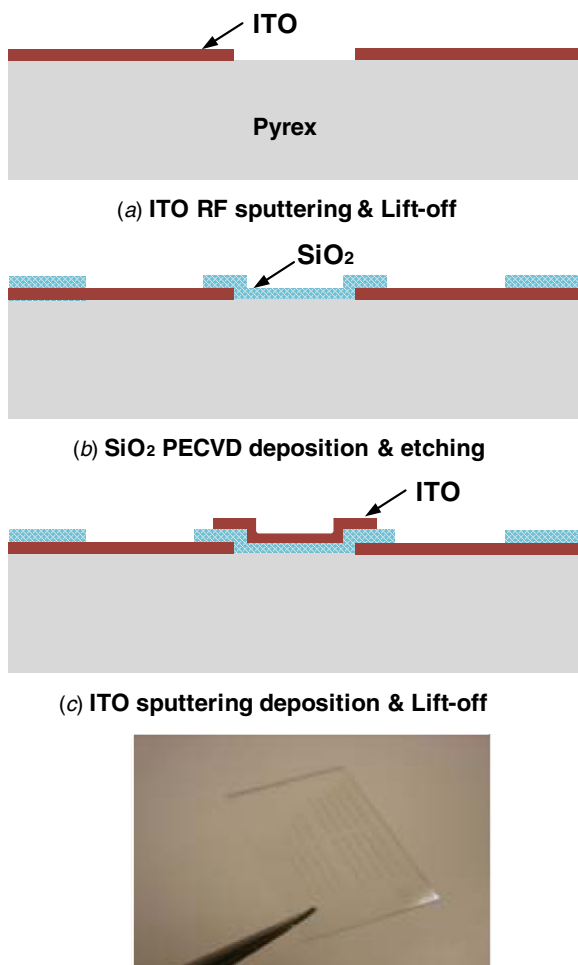


**Figure 2.** Fabrication process of the proposed platform. (a) Deposition of the first layer of ITO using the lift-off process to define electrodes, contact pads and interconnections. (b) Silicon dioxide layer deposition and patterning. (c) Second ITO layer deposition and patterning. Bottom: optical photo of fabricated platforms under visible light.

layer was measured as 20–25  $\Omega/\square$ . The lower resistivity is preferred for lower activating voltages in electrochemical treatment. As the resistivity can vary from device to device, having device process in stable condition is important and acquiring corresponding activating voltage is required for each device fabrication run. Without the annealing process, the electrochemical activation process was not repeatable probably due to poor electrical properties. Afterward, a layer of 150 nm-thick silicon dioxide was deposited at 200 °C by PECVD (plasma-enhanced CVD) and patterned with dry etching as shown in figure 2(b). The reason for using low-temperature PECVD is to minimize the thermal effect on ITO layers. The second, 150 nm-thick ITO layer was deposited and defined by sputtering and patterning using lift-off as illustrated in figure 2(c). Annealing the device at 350 °C for 1 h completed the fabrication process. The total thickness of the device was about 300–350 nm. That barrier height was overcome without problem in the test by MDCK (Madin Darby canine kidney) and NIH 3T3 cells' mobility. Also, Pyrex, silicon dioxide and ITO are all optically transparent

to visible light so that the fabricated device was optically transparent as shown in the bottom photo of figure 2. The wafers were diced into devices of typical size 8 mm  $\times$  12 mm for easier manipulation afterward.

### 2.3. Surface treatment for the control of cell attachment

Polyethylene glycol (PEG) silane purchased from Gelest has been widely used for its non-toxic property with the possibility of versatile functionalities. PEG with silane treatment used in this study creates strong bonding with the ITO surface [16]. Previously, static cell patterning and cell co-culture were demonstrated using PEG silane treatment on the ITO surface [8] and the corresponding recipe was modified in this study as illustrated in figure 3. First, microfabricated platforms were cleaned with oxygen plasma at 150 W for 1 min. The purpose of the oxygen plasma was to remove any organic residues on the surface and also to introduce hydroxyl groups that can bind with PEG silane. The platforms were dipped into 1% v/v of PEG silane dissolved in anhydrous toluene for 6 h. During this process, the surfaces of ITO, Pyrex and silicon dioxide were grafted by PEG-silane to establish hydrogen and covalent bonds. The subsequent curing process for 90 min at 120 °C on a hot plate (in contrast to a hot oven in the original recipe) was followed to secure the covalent bond and to transform the weak hydrogen bond to covalent bond through the chemical condensation process. The platforms were stored in the vacuum desiccator to prevent contact with moisture. The removal of covalently bonded PEG silane from the surface was based on electrochemical desorption [8, 14]. The PEG-silane desorption process was conducted in a 1 $\times$ PBS (phosphate buffered saline) solution or culture media (DMEM) for the formation of electrically closed loop circuit. The applied potential was  $-1.5$  V for 45 s (in contrast to  $-1.4$  V and 60 s in the original recipe) in this study and the reference probe was placed about 5 mm away from the ITO surface. PEG-silane on top of the electrically insulating Pyrex and silicon dioxide surfaces was not affected in this process and only the PEG-silane on the electrically-activated ITO surface was removed.

The PEG coating on the surface and the desorption of PEG-silane from the ITO surface can be verified by various methods such as XPS (x-ray photoelectron spectroscopy), AFM (atomic force microscope), fluorescent imaging method or contact angle measurement [8, 15]. The long chain structure of PEG has been known to exhibit a hydrophobic property and the contact angle measurement was used in this work to validate the PEG surface coating process. In all contact angle tests, at least ten experiments were conducted for each surface characterization. The initial water contact angle without surface treatment was measured as  $23 \pm 4^\circ$  on the bare ITO surface. After the PEG silane passivation, the contact angle increased to  $64 \pm 4^\circ$ , indicating successful surface modification with the long chain structure of PEG. After the PEG-silane desorption process, a contact angle of  $31 \pm 4^\circ$  was observed. Clearly, the contact angle was not able to return to the original value of the bare ITO surface probably due to the contributions of residual PEG-silane. The average

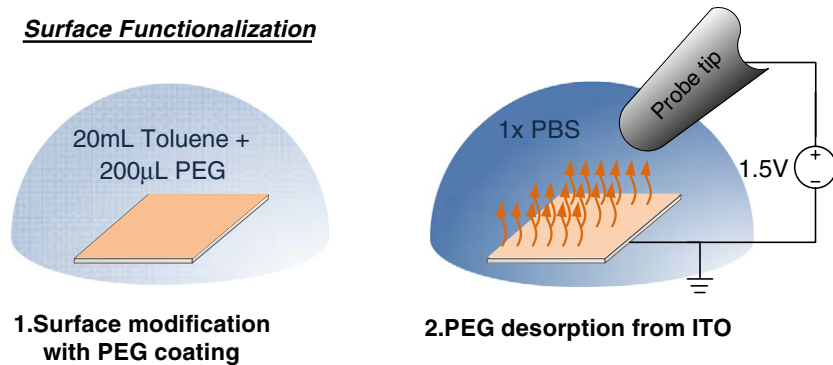


**Figure 3.** Left: the composition of 1% v/v PEG silane dissolved in anhydrous toluene was used to form the hydrogen bond with the platform surfaces (ITO, Pyrex and oxide) and the subsequent condensation process transforms the hydrogen bond to the covalent bond. Right: activation of the selective ITO electrode was performed in culture media by applying  $-1.5$  V potential to the ITO electrode.

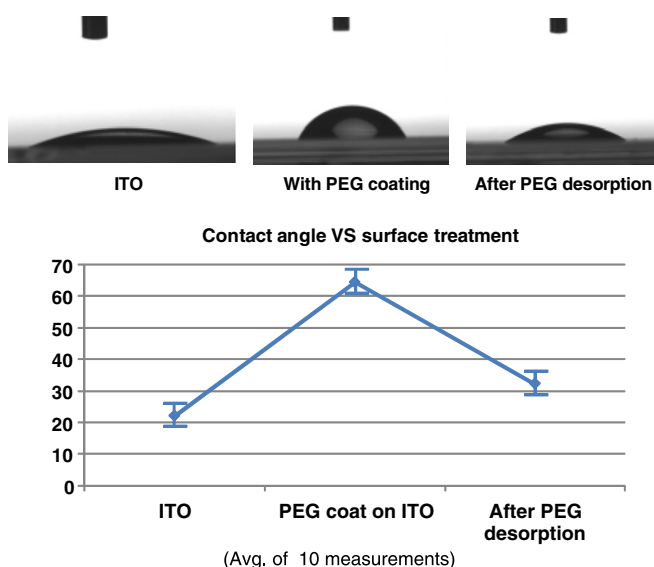


**Figure 4.** Contact angle is measured on the ITO surface before PEG coating, after PEG coating and after PEG desorption. As the long chained PEG shows hydrophobic property, the contact angle increased after PEG coating and the desorption of PEG effectively reduced the contact angle.

measurement result is plotted in figure 4 with corresponding optical images.

### 3. Dynamic cell co-culture test results

#### 3.1. Static cell patterning and preliminary cell-to-cell co-culture test

A fabricated platform was first dipped into the  $1 \times$  PBS solution for selective activation of ITO on one specific electrode and NIH 3T3 cells with concentration of  $5 \times 10^5$  cells  $\text{ml}^{-1}$  were added on top of the platform. After 1 h for cells to settle and seat on the surface, a flushing process was conducted to remove loosely attached cells. Optical and fluorescent images were taken 36 h after the flushing process as shown in figure 5. Figure 5(a) shows no cell attachment on the electrode without using the electrochemical activation process, while figure 5(b) shows cell attachment and growth

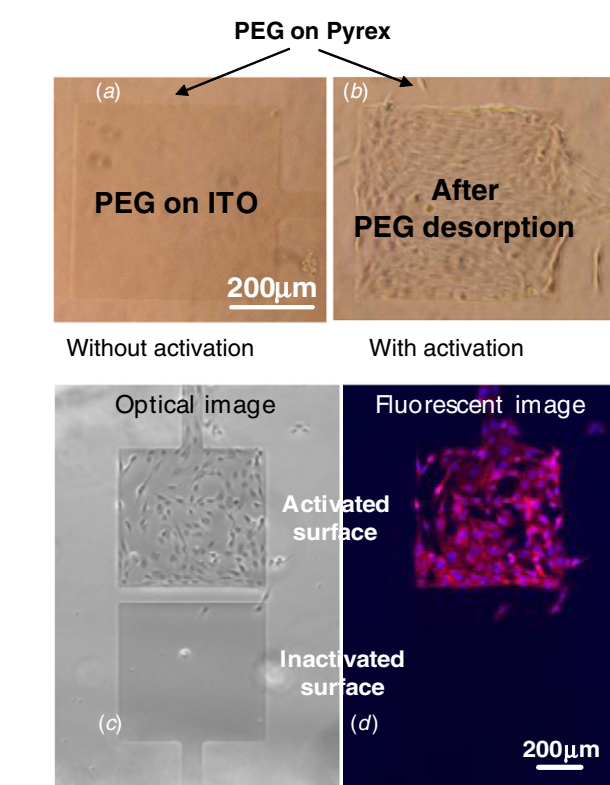


**Figure 5.** Optical photos showing the patterning of NIH 3T3 cells. (a) No living cells were found on the electrode ( $500 \mu\text{m} \times 500 \mu\text{m}$ ) without the electrochemical activation process. (b) Living cells were able to seat on the activated ITO electrode. (c) An optical photo showing the comparison between activated (top) and inactivated electrodes. (d) Florescent image of (c).

on the activated ITO electrode. Figures 5(c) and (d) are optical and fluorescent images 24 h after the flushing process, respectively. They demonstrate clearly that electrodes with and without electrochemical activation can and cannot have cell growth on the surfaces.

The feasibility to control two types of cells to interact in a controlled manner in space and time is based on one fundamental assumption in our setup: the seating of second-type cells will not react with the first-type cells prematurely. Otherwise, the second-type cells can grow on top of the

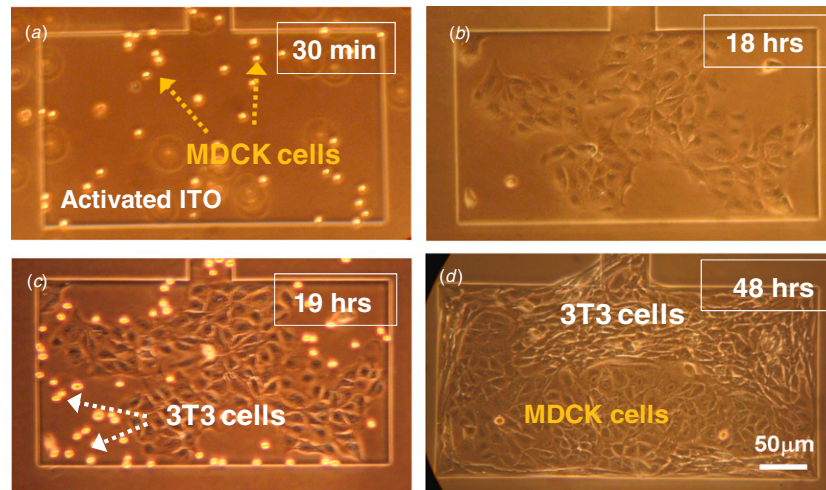


**Figure 6.** MDCK and NIH 3T3 cell lines were cultured in the MEMS platform for feasibility study. (a) 30 min after the loading of the MDCK cells on an activated electrode. (b) 18 h into the experiment, proliferation of MDCK cells was observed. (c) NIH 3T3 cells were loaded at the 18th h and they were seated on the open space of the activated electrode in this 19th h optical photo. With the flushing process, loosely attached NIH 3T3 cells on both the inactivated electrode and top of MDCK cells were removed. (d) After 48 h into the experiment, NIH 3T3 cells and MDCK cells had proliferated to fill up the activated electrode.

first-type cells and mess up the characterization of real cell-to-cell interactions. To validate the feasibility of the proposed platform, the following experiment was conducted. First, the platform is coated with PEG silane and one ITO electrode is activated. Figure 6(a) shows 30 min after the loading, seating and washing of MDCK cells. These cells were sitting only on the activated electrode area. After 18 h into the experiment, MDCK cells were able to spread out only on the electrode as seen in figure 6(b). NIH 3T3 cells were added into the culture media afterward. Figure 6(c) is the optical photo showing the seating of 3T3 cells 1 h after the seating process or 19 h into the overall experiment. It was found the NIH 3T3 cells were able to attach only onto the electrode with open spaces and not on top of the MDCK cells. It was observed that NIH 3T3 cells that were sitting on top of the MDCK cells were easily detached during the post flushing process with the PBS solution. Figure 6(d) shows results after 48 h into the experiment and these two types of cells were grown together and filled up the activated electrode area. This experiment validates the basic assumption for the proposed MEMS platform that the second-type cells may easily attach to the open surface and not onto the first type of living cells that were already seating on the electrode during the flushing process.

### 3.2. Two types of cells for cell-to-cell co-culture experiments

NIH 3T3 and MDCK cells were used in the prototype demonstration because they are two of the most representative cell lines among fibroblast and epithelial cells, respectively. Figure 7 shows the dynamic cell-to-cell co-culture protocol used in this work and corresponding test results. Figure 7(a) illustrates time and space control in the following three steps: (1) surface activation of the first electrode (left) and loading and proliferation of the MDCK cells, (2) surface activation of the third electrode (right) and loading and proliferation of

the NIH 3T3 cells, and (3) surface activation of the center electrode. Sequential images of the test results are shown in figures 7(b)–(g) with corresponding time span. After 18 h of culture with  $5 \times 10^5$  cells  $\text{ml}^{-1}$  of MDCK cells in the initial loading process, figure 7(b) shows mostly the full spreading of MDCK cells on the left electrode while the other electrodes/areas were not covered by the cells. After 23 h into the experiment, the right electrode was electrochemically activated and NIH 3T3 cells with concentration of  $2.5 \times 10^5$  cells  $\text{ml}^{-1}$  were loaded. The flushing process was conducted 1 h afterward (24 h into the experiment) and the result was shown in figure 7(c). NIH 3T3 cells could sit on various open surfaces on the platform but they could be easily washed away during the flushing process as the cell adhesion to the inactivated surface was weak. Very limited NIH 3T3 cells were observed on the left and center electrode areas but they were not able to seat and grow as observed in the next optical photo of figure 7(d). Figure 7(d) shows results 40 h into the experiment with successfully cultured MDCK and NIH 3T3 cells on each electrode, respectively. In this stage, the cells on both sides are not able to migrate into the center electrode. The center electrode was activated at the 40th h to allow migration of cells into the center electrode while overcoming the barrier gap. Figure 7(e) shows the optical photo of cell migrations into the center electrode while some open space can still be observed. Continuous migration and proliferation of the cells make the activated electrode areas confluent 80 and 100 h into the experiment as shown in figures 7(f) and (g), respectively. It is observed that up to 100 h of total culture time, the living cells were confined in the activated electrode areas, while slight outgrowth of the cells over the activated electrode areas started to occur in figures 7(f) and (g). Surface coating of PEG silane diminishes due to constant exposure to the culture media and 100 h was a good stopping point for the cell-to-cell co-culture experiment without the severe outgrowth of living cells.

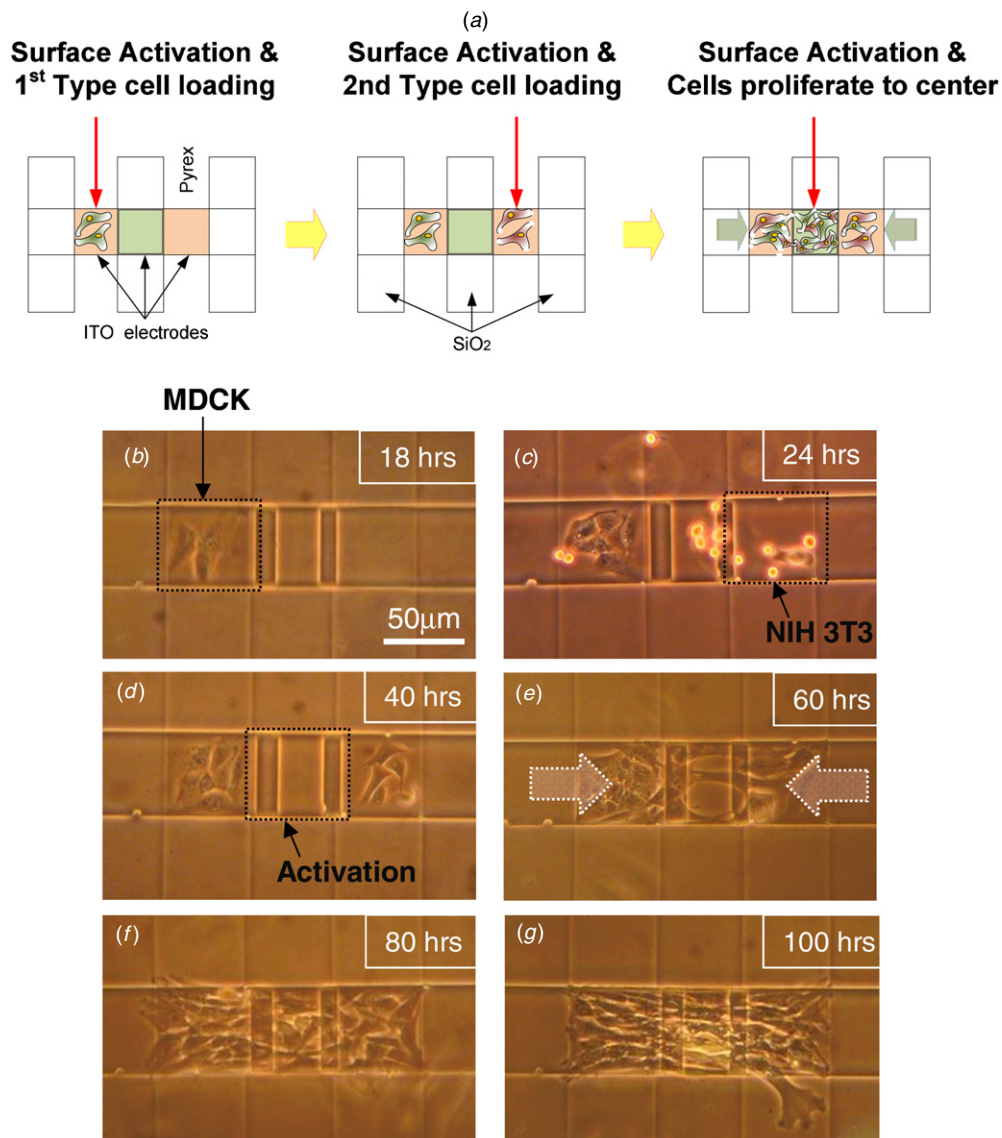


**Figure 7.** (a) Schematic diagram illustrating the procedures of the dynamic cell-to-cell co-culture tested by the sequential activation of electrodes and subsequent cell loadings. (b) First, the left electrode was activated and the MDCK cells were loaded and the photo was taken 18 h into the experiment. (c) 23 h into the experiment, the right-side electrode was activated and NIH 3T3 cells were loaded. The photo was taken 24 h into the experiment and most NIH 3T3 cells were sitting only on the activated right electrode. (d) 40 h into the experiment, the center electrode was activated. (e) Migrations of both cells into the center electrode were observed 60 h into the experiment. Some open space can still be observed on the center electrode. (f) 80 h into the experiment, the two cell lines cover almost the whole areas of the three activated electrodes. (g) 100 h into the experiment, some outgrowth of cells over the activated electrode areas was observed.

#### 4. Discussion

The key feature of surface modification is based on strong adhesion between ITO and PEG-silane. Several key processes are crucial to achieve strong adhesion: (1) uniform coating of PEG-silane on the surface, and (2) enough time for the soaking process in the PEG-silane dissolved solution. For example, non-uniform coating and failure of PEG passivation have been found on the ITO surface due to the lack of PEG-silane soaking time. Curing under proper temperature is also known to help change the hydrogen bond to covalent bond through the condensation process. Experimentally, it is found that the MEMS platform should not be exposed to the air or moisture environment for strong PEG silane passivation. Therefore, these MEMS platforms have been placed in a

nitrogen incubation chamber during the various steps of the fabrication processes and stored in the vacuum desiccator after the completion of the process to avoid degradation of PEG. Furthermore, it was found that a 60 s electrochemical activation process caused darkened color of the ITO surface which affected the transparency of the platform. The 45 s activation time used in this work was found adequate to accomplish the purposes of both activation and optical transparency.

The structural pattern is crucial to constrain cells on defined electrode areas. Figure 8 shows a typical electrode which has both acute angles (smaller than  $180^\circ$ ) and obtuse angles (over  $180^\circ$ ) on the corners of the patterned structure. It is observed that cells were able to protrude from both sides of the corners with obtuse angles—the dotted line was the

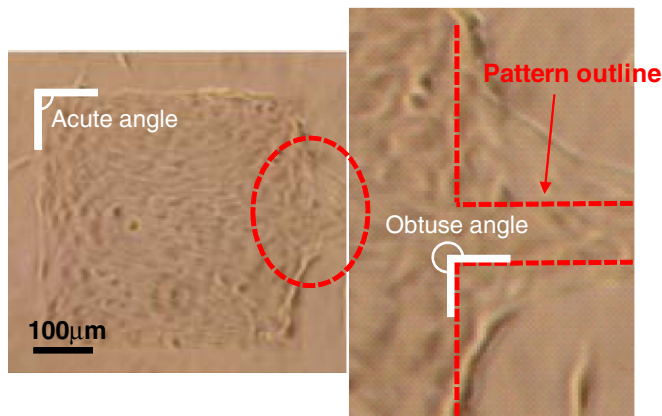


**Figure 8.** When structures have obtuse angle features it is hard to confine cells on patterned electrodes due to strong affinity between cells. On the other hand, structures with acute angles seem to be able to confine the outgrowth of cells.

electrode pattern. However, cells were well confined for the case of corners with acute angles. Therefore, acute angle corners are preferred for cell cultures that require a high degree of confinement.

Gap control is also critical as the barrier has to be small enough for the cells to overcome for migration and cell-to-cell co-culture but large enough to have repeatability in device fabrication. The 2  $\mu\text{m}$  gap realized in this study was shown to be adequate for both tested cell lines as both cells were able to migrate over the gaps. However, further investigations on the minimum gap sizes with respect to different types of cell lines should be conducted as design guidelines for future cell-to-cell co-culture studies. Furthermore, the current fabrication process could be easily scaled up to 2D arrayed patterns by utilizing the first ITO layer as electrical connection lines at the bottom of the platform and the second ITO layer as the functional electrodes.

Finally, other cell patterning schemes could provide longer experimental period for cell-to-cell co-culture studies. Results presented in this project using PEG silane could provide good surface protection up to about 100 h. Outgrowth of the cells was easily observed after 100 h. Although this platform is capable of accommodating the growth of multi-types of cells on the single substrate, the time required for one type of cell to fully occupy the activated electrode area is long. As a result, the time requirements for the sequential loading process severely limit the possible number of different types of cells to be loaded for studies. One possible solution is a parallel loading process probably accomplished by means of microfluidics [17] by delivering different types of cells to different electrodes simultaneously. Nevertheless, the platform presented here demonstrated the feasibility of multicellular cell-to-cell co-culture experiments with both spatial and temporal controls.

## 5. Conclusion

In this work, we present a MEMS-based biological platform designed for dynamic cell patterning with multi-types of cell-to-cell co-culture based on the electrochemical activation

of ITO. Serial and selective activation as well as optical transparency are combined into a single platform to realize cell-to-cell co-culture experiments with both spatial and temporal controls. The surface of the device is grafted with PEG-silane to prevent cell adhesion and growth and the PEG layer on individual electrodes can be removed selectively to allow loading of living cells sequentially. It is found that electrochemical desorption of the PEG-silane can be effectively restored to hydrophilic as shown in the contact angle experiments. The proposed biological platform has been verified to control the position of living cells in time and space. Furthermore, dynamic cell-to-cell co-culture tests using MDCK and NIH 3T3 cell lines have been performed. As such, it is believed that the proposed biological platform can help exploring and revealing biological insights of transient and dynamic cell-to-cell interactions with these simple yet versatile platforms.

## References

- [1] Britland S, Clark P, Connolly P and Moores G 1992 Micropatterned substratum adhesiveness: a model for morphogenetic cues controlling cell behavior *Exp. Cell Res.* **198** 124–9
- [2] Healy K E, Thomas C H, Rezaia A, Kim J E, McKeown P J, Lom B and Hockberger P E 1996 Kinetics of bone cell organization and mineralization on materials with patterned surface chemistry *Biomaterials* **17** 195–208
- [3] Lahann J, Choi I S, Lee J, Jensen K F and Langer R 2001 A new method toward microengineered surfaces based on reactive coating *Angew. Chem., Int. Ed.* **40** 3166–9
- [4] Liu W F and Chen C S 2005 Engineering biomaterials to control cell function *Mater. Today* **8** 28–35
- [5] Tan J L, Liu W, Nelson C M, Raghavan S and Chen C S 2004 Simple approach to micropattern cells on common culture substrates by tuning substrate wettability *Tissue Eng.* **10** 865–72
- [6] Delamarche E, Bernard A, Schmid H, Michel B and Biebuyck H 1997 Patterned delivery of immunoglobulins to surfaces using microfluidic networks *Science* **276** 779–81
- [7] Yamato M, Konno C, Utsumi M, Kikuchi A and Okano T 2002 Thermally responsive polymer-grafted surfaces facilitate patterned cell seeding and co-culture *Biomaterials* **23** 561–7
- [8] Shah S S, Lee J Y, Verkhoturov S, Tuleuova N, Schweikert E A, Ramanculov E and Revzin A 2008 Exercising spatiotemporal control of cell attachment with optically transparent microelectrodes *Langmuir* **24** 6837–44
- [9] Hui E E and Bhatia S N 2007 Micromechanical control of cell–cell interactions *Proc. Natl Acad. Sci. USA* **104** 5722–6
- [10] Li Y, Yuan B, Ji H, Han D, Chen S, Tian F and Jiang X 2007 A method for patterning multiple types of cells by using electrochemical desorption of self-assembled monolayers within microfluidic channels *Angew. Chem., Int. Edn.* **46** 1094–6
- [11] Lee E J, Chan E W L and Yousaf M N 2009 Spatio-temporal control of cell coculture interactions on surfaces *ChemBioChem* **10** 1648–53
- [12] Chang J, Yoon S H, Mofrad M R K and Lin L 2010 MEMS-based biological platform for dynamic cell-to-cell interaction characterization *Proc. 23th IEEE Micro Electro Mechanical Systems Conf. (Hong Kong, January 2010)* pp 92–5
- [13] Sochol R D, Higa A T, Janairo R R R, Chou A, Song L and Lin L 2009 Unidirectional cellular durotaxis via

- microfabricated posts of varying anisotropy *15th Int. Conf. on Solid-State Sensors, Actuators and Microsystems (Denver, CO, June 2009)* pp 604–7
- [14] Tang C, Feller L, Rossbach P, Keller B, Vörös J and Tosatti S 2006 Adsorption and electrically stimulated desorption of the triblock copolymer poly(propylene sulfide-bl-ethylene glycol) (PPS-PEG) from indium tin oxide (ITO) surfaces *Surf. Sci.* **600** 1510–7
- [15] Razunguzha T, Warriar M and Timperman A T 2006 ESI-MS compatible permanent coating of glass surfaces using poly(ethylene glycol)-terminated alkoxy silanes for capillary zone electrophoretic protein separations *Anal. Chem.* **78** 4326–33
- [16] Schlapak R, Armitage D, Saucedozeni N, Hohage M and Howorka S 2007 Dense passivating poly(ethylene glycol) films on indium tin oxide substrates *Langmuir* **23** 10244–53
- [17] Rhee S W, Taylor A M, Tu C H, Cribbs D H, Cotman C W and Jeon N L 2005 Patterned cell culture inside microfluidic devices *Lab Chip* **5** 102–7